Feb. 7, 1994

Progress Report for NASA Grant NAG 5-1244

/3769

// P

The following is a summary of our work in the last six months or so, since the last progress report. We have made a great deal of progress in this time period, and are finally getting some good x-ray detection data. We feel the "proof of concept" stage has been attained, and we need only perform minor modifications to develop a usable device. Lower temperatures seemed to be the key to achieving better x-ray response, and we were finally able to lower the temperature to verify this statement. Our NASA collaborators have loaned us a 2-stage pumped ^{3}He dewar which gets us down to about 0.3 K. It is anticipated that some modifications to the dewar will further decrease this temperature to around 0.25 K. As mentioned below, the decrease in temperature really makes a huge difference.

Device Status

We are still using the mask set generated at Cornell's NNF last year. These devices are not quite ideal, but do still offer good promise as effective x-ray detectors. We have switched back to an iron chloride – based wet etch for the Ta absorber definition. This is to give sloped sidewalls on the thick Ta, hopefully resulting in better edge coverage in the subsequent Al trap deposition. We are very careful with the rinse after the Fe etch, but are still a bit concerned about Fe precipitates remaining at the Ta surface. This issue is secondary, and will only be examined in the future, as it has not proven detrimental to our x-ray detection efforts.

We have done some other testing of Ta film quality on various substrates. We currently use thermally oxidized ($\approx$3000 Å oxide) silicon wafers as substrates, and consistently get residual resistance ratios (RRRs) of 16 to 20 (this for Ta deposition at 650° C, approximately 10^{-7} torr background at 650° C, and sputtering rate of $\approx$35 Å/s). The amorphous silicon oxide layer on the substrate is advantageous because it scatters ballistic phonons -- keeping substrate absorptions from sending a large portion of their energy into the Ta absorbers or Al traps. This should aid in ensuring that all x-ray pulses we see come from Ta absorption locations -- and will therefore increase the energy resolution of the detector. We have also done a small amount of work with Ta deposited on single crystal MgO substrates. Preliminary tests show RRRs as high as 30 or more! It will be important to determine which is more necessary: an amorphous substrate layer, or increased quasiparticle mean free path in the Ta.

Our devices show nearly ideal BCS characteristics even down to our lowest (0.3 K) temperatures -- particularly at low voltages. At higher voltages, near one delta, we still have excess current which exhibits an exponential-like rise as in an S-I-N type of tunnel junction. Figure 1 shows this rise on the blue (I x 500) curve (note the magnetic field is used to suppress the Josephson current, and does so very effectively). There are a few ideas we have for reducing this excess current, as it is detrimental to our S/N ratio (lower dynamic resistance gives larger noise gain in the charge sensitive preamp). Firstly, we will try cooling the devices somewhat slower through the superconducting transition. (There is some evidence that thermoelectrically generated currents from excessive temperature gradients can result in trapped flux in or near the tunnel junction.) We will also pay closer attention to the substrate temperature during device fabrication. The final SiO and Al layers on the device are deposited by thermal evaporation. It is likely that radiated heat from these sources can significantly heat the devices, and there is evidence that even mild heating can be harmful to Al junction devices. A copper block attached to the back of the devices with vacuum grease should help alleviate any such problems. (We have been using a copper block without any grease, but it is not clear the thermal contact to the substrate is good enough.) Finally, if none of this works, we might substitute e-beam evaporated Al_2O_3 for the SiO. This could help alleviate potential leakage problems near the junction edges due to poor stoichiometry of the evaporated SiO.

Electronics

With a *current* sensitive amplifier, we were able to observe alpha particles and x-rays at 0.36 K. Unfortunately, the peak height of such amplified pulses is very dependent on x-ray absorption event location (pulses closer to the junction give faster rise times, and thus give higher effective current pulse heights). Therefore, we switched to a *charge* sensitive preamp, which effectively integrates the current pulse to remove any absorption position dependence. This preamp is not matched well by junction dynamic resistances less than a kilohm or so -- and thus requires lower temperature junctions. Our 200 ohm 0.36 K junctions became 2 kilohm at 0.30 K, and were very stable and relatively low noise when coupled to the charge sensitive preamp. There still needs to be a factor of about 5 increase in dynamic resistance before we are near an optimum situation for the preamp. Lower temperatures (0.25 K, for example) might help. We are also in the process of getting new photomasks from Cornell NNF, which have slightly improved device designs -- including smaller junction areas (by a factor of 2 or 4). This will also help raise the dynamic resistance of the devices.

Photon Detection

At 0.30 K, we see excellent S/N ratios for our x-ray pulses, within a factor of 5 for what is necessary in a final device. Figure 2 shows a typical pulse (at the output of the charge sensitive preamp). This is the integrated charge from a *single* 6 keV x-ray. The S/N ratio is approximately 100, and the total collected charge is of order 10^7 electrons. The amount of collected charge is among the largest seen by any other group, and gives hope that these devices will replace semiconducting detectors in the near future. (If you recall, the statistical broadening in the energy resolution of a detected x-ray obeys a normal distribution, going like the square root of the number of particles produced. For a 6 keV x-ray, one would expect approximately 3000 charges produced in a Si detector. We have about 3000 times more charges produced in our superconducting tunnel junction detector, and therefore potentially about 50 times better resolution.)

Figure 3 displays a histogram (red curve) of the "collected charge in a pulse" vs. "number of counts at that collected charge" (there are 200 horizontal "bins" in this figure). The amount of collected charge is related very nearly linearly to the deposited x-ray energy. There are a few things to note in this figure:

1) the very large peak down near zero collected charge is a measure of the baseline noise of the electronics (i.e., it is not from x-rays); this gives us about 50 eV as a minimum energy resolution due to electronic noise. With increased junction dynamic resistance, and eventually reduced device capacitance, this value can realistically be reduced by a factor of ten.

2) The peak at approximately 8 million electrons collected exhibits a relatively sharp rise on its low energy side. This indicates that substrate (rather than in the superconducting films) absorption events do not cause much degradation in energy resolution -- if this were not true, one would expect to see a large "background" component with increasing amplitude as the number of collected electrons goes to zero. (Note that the discrimination level -- to window out unwanted "noise" pulses -- only allows pulses with more than about 2 million electrons.) The low substrate component indicates that our idea to use thermally oxidized Si substrates is a good one. The amorphous oxide on the Si is utilized to scatter any ballistic phonons coming from substrate absorptions. The phonons that do make it through this layer and into the superconducting films are then of low enough energy that they do not result in any significant signal at the tunnel junction.

3) There is an anomalous component to the peak at higher collected charge. Based on the amount of collected charge, and the electronic noise component, we should see a peak with only about 50 eV full-width at half-maximum (FWHM). Instead, we see a peak fit relatively well by a gaussian (black curve in Figure 3) with 350 eV FWHM, and a great deal of straggle at higher energies. As discussed below, we believe this excess component is due simply to our electronics, and should be correctable.

Figure 4 is the histogram of pulse risetimes from the same data set. By "risetime," we mean the actual fall time of the pulses as shown in Figure 2 (10% - 90%). One important point to note on this figure is the magnitude of the risetimes, with a peak near 20 μs. Based on considerations involving quasiparticle backtunneling through the junction, we can use this 20 μs value as an estimate for the quasiparticle lifetime in Al at 0.3 K. This is in very good agreement with theory and with previous experiments by other researchers. Note also that due to the huge number of quasiparticles produced (as inferred from the amount collected), self-recombination (among quasiparticles produced by the x-ray rather than the thermal background) is becoming a significant effect. The quasiparticle density created in the Al trap by a 6 keV x-ray is approximately equal to that of the thermal background at 0.3 K. This tells us that lower temperatures are not going to help us much in terms of lengthening relevant quasiparticle lifetimes. In addition, it is not clear that lower temperatures will help us much in terms of lowering the noise signal (we want higher dynamic resistance, but an x-ray pulse gives us a certain lower dynamic resistance for the short time we have the generated quasiparticles in the tunnel junction area -- and this value will apparently be approximately independent of temperature below a given temperature ≈ 0.3 K). Thus, it is not clear that dilution refrigerator temperatures will benefit us any more than 0.25 K from the 2-stage ^{3}He dewar, but it is clear that we need to work on maximizing the dynamic resistance of the tunnel junctions for temperatures around 0.3 K (possibly using the techniques mentioned above).

Using Figure 4 along with the total charge collected (as given in Figure 3), we can also estimate a lower bound for the quasiparticle lifetime in Ta. The collected charge of about 10^7 electrons is approximately 15% of the maximum charge we could expect to collect (this estimate includes the effects of backtunneling, but does not make any correction for charge losses due to the electronics as discussed below). Therefore, the losses in the Ta cannot be any more than 85%. Given quasiparticle trapping times (to get the quasiparticles out of the Ta, and into the long lifetime Al) of order 0.5 μs, an 85% quasiparticle loss before trapping would necessitate a lifetime of 250 ns. This is a *lower bound*, as we have made no attempt to correct for quasiparticle losses due to incomplete multiplication upon trapping, and due to the electronics. Consideration of these ignored effects could plausibly give Ta quasiparticle lifetimes of as much as 100 μs, but we will not know until we can perform tests with double tunnel junction geometries (see future plans, below).

In Figure 4 we also see a good deal of straggle towards shorter (faster) risetimes. We believe that x-ray absorption events in or near the quasiparticle trap (rather than in the Ta absorber) cause a faster signal risetime. This can simply be due to the created quasiparticles being closer to the tunnel junction, or it can involve more complicated effects where our high frequency voltage bias point changes in such a way as to increase the tunneling rate. In any case, an interesting test involves using software to window out the pulses with risetimes faster than about 19.5 μs. Figure 5 shows the resulting histograms after the windowing out of fast pulses. The very high energy straggle has disappeared. In addition, the peak has become somewhat sharper, with FWHM now of about 230 eV. This is only a factor of 2 worse that state-of-the-art semiconductor detectors, and indicates we are well on the way to producing truly useful devices. We believe that some minor modifications to the electronics will take us a long way in improving this FWHM.

The fast pulses are correlated with large collected charge. This correlation can be explained by a charge loss mechanism with a time constant of about 20 μs. Fast pulses will build up to their maximum value before the loss mechanism kicks in, while slow pulses will continually lose charge before they have even deposited it fully in the charge integrator. We propose that this "loss" mechanism is actually due to nonidealities in the op-amp-like integrator we use for the charge

Note: the discussion at the beginning of this paragraph and the conclusion as to the source of the long pulse risetime have been superceded by the treatment on pages 93-5 of Michael Gaidis' Ph.D. thesis. Copies of this thesis are with Dr. Szymkowiak and Dr. Moseley of GSFC.
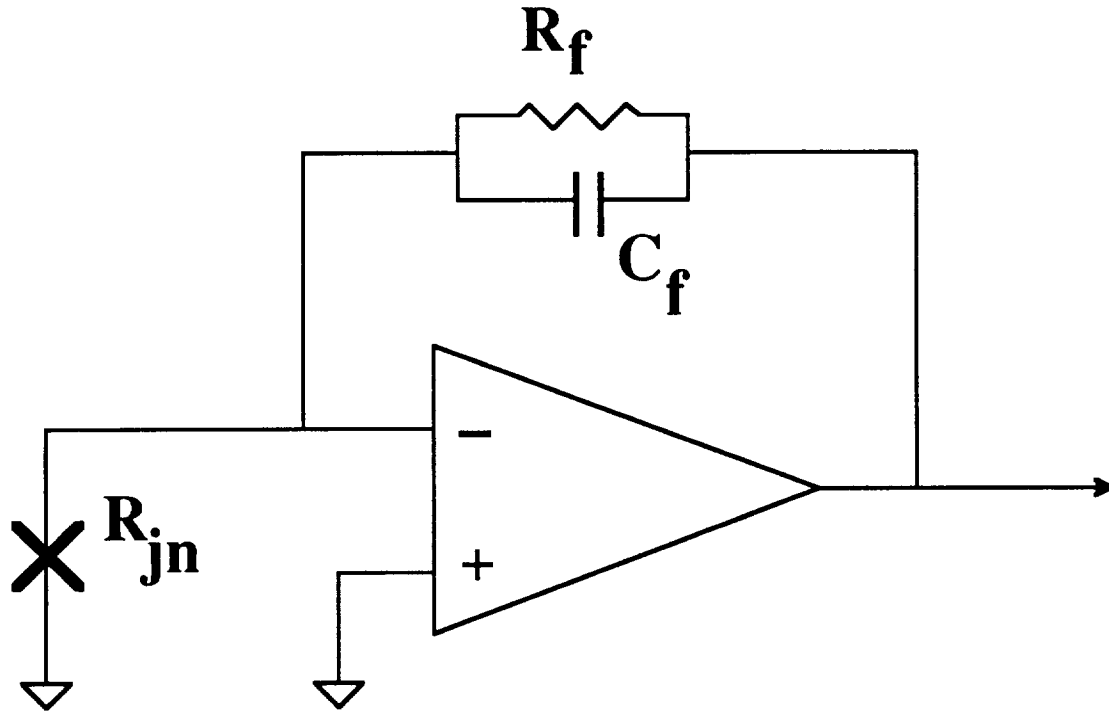
June 30, 1994

Figure 6: Simplified charge integrator schematic.

collection. Figure 6 is a simplified schematic of our charge integrator. The charge produced in the junction is deposited on the feedback capacitor (10 pF in our case), and the output voltage is given simply by the relation $V=Q/C$. For an ideal op-amp, the charge would leak off the feedback capacitor with time constant R_fC_f (≈ 100 µs in our case). However, because the open loop gain of the op-amp is not infinite, there is a nonzero voltage at the inverting terminal of the op-amp. This causes current to flow through the junction (leaking off of the feedback capacitor). The time constant for such leakage is given by $R_{jn}C_fA_{ol}$, where A_{ol} is the open-loop gain of the op-amp at the frequency corresponding to a time constant $R_{jn}C_{jn}$. In our arrangement, $R_{jn}C_{jn}$ is typically about (2000 ohms * 200 pF) = 0.4 µs (or, f $\approx$ 0.5 MHz). At this frequency, a realistic estimate for A_{ol} is 1000, thus giving $R_{jn}C_fA_{ol} \approx 20$ µs.

Is this really our loss mechanism?   Figure 7 lends some support to this theory. It is a plot of collected charge vs. risetime, with each individual pulse represented by a single dot. The blue points (at slower risetime) are taken at a particular dc bias point (giving approximately 2000 ohms dynamic resistance); the red points are at a different bias (approximately 800 ohms dynamic resistance). The trend is clear, and fits well with the explanation.

If this is indeed our "loss" mechanism, it is obvious what we can do to remove it: increase R_{jn}, C_{jn}, C_f, or A_{ol} such that $R_{jn}C_fA_{ol} \approx 100$ µs. Unfortunately, we are restricted somewhat in what we can do: increasing C_{jn} to indirectly increase A_{ol} will increase high frequency noise gain; increasing C_f will decrease the closed-loop gain of the integrator, making it potentially less stable; increasing A_{ol} is certainly feasible, but is difficult: the high bandwidth amplifiers necessary for such high gain at 0.5 MHz tend to be hard to stabilize, especially since they must be stable for near-unity noise gain at very high frequencies. The only option without any drawbacks is increasing R_{jn}.

Future Plans

To sharpen the peak on the collected charge histogram, we will concentrate on increasing R_{jn} and A_{ol}. Ideas for increasing R_{jn} are mentioned above, and A_{ol} can possibly be increased by using

4

an extra FET inside the integrator loop, or by using some different op-amps (namely, Burr-Brown's new 642 is an excellent, high bandwidth, low noise, unity-gain stable op-amp). A more tricky solution is to play with the closed-loop gain to increase it at higher frequencies so a unity-gain stable op-amp is not necessary.

With the recent success in pulse detection, we are ready to move to double junction geometries. In these structures, a single Ta absorber strip is common to tunnel junctions at two of its edges. In this way, we can detect a single x-ray simultaneously at two different junctions. The relative pulseheights of the junctions for a single x-ray give spatial resolution on the absorption position. This pulseheight #1 vs. pulseheight #2 data can also be fit to a model incorporating loss mechanisms in the Ta, giving us an estimate for the relevant quasiparticle recombination time in the Ta, and allowing us to correct for it with software.

The progress in this project seems to be increasing at an exponential pace. It is a very exciting time for such detectors, and we have even more confidence now that these detectors will eventually surpass the performance of the best semiconductor detectors -- by enough to make even the cryogenic operating temperatures practical.

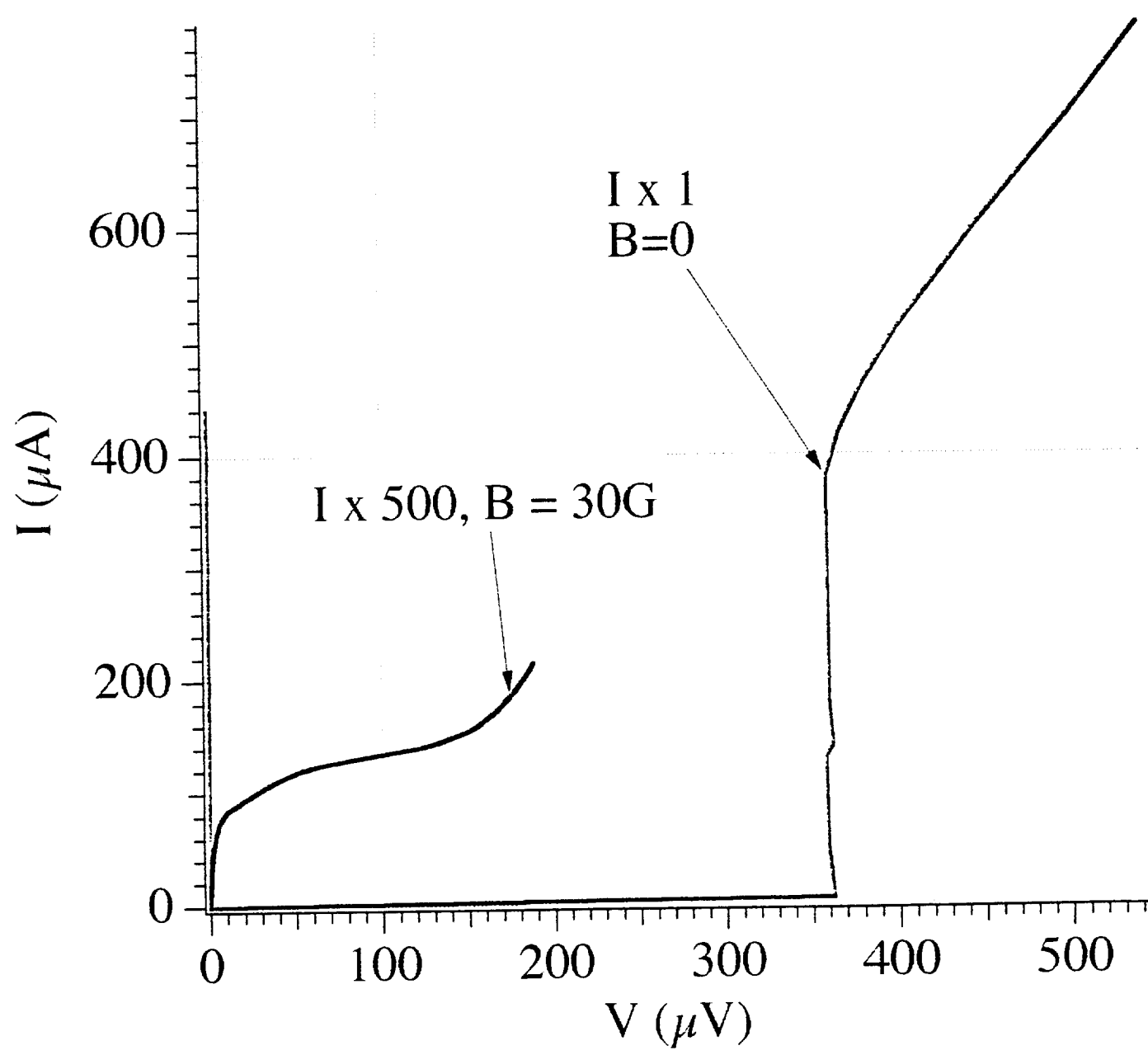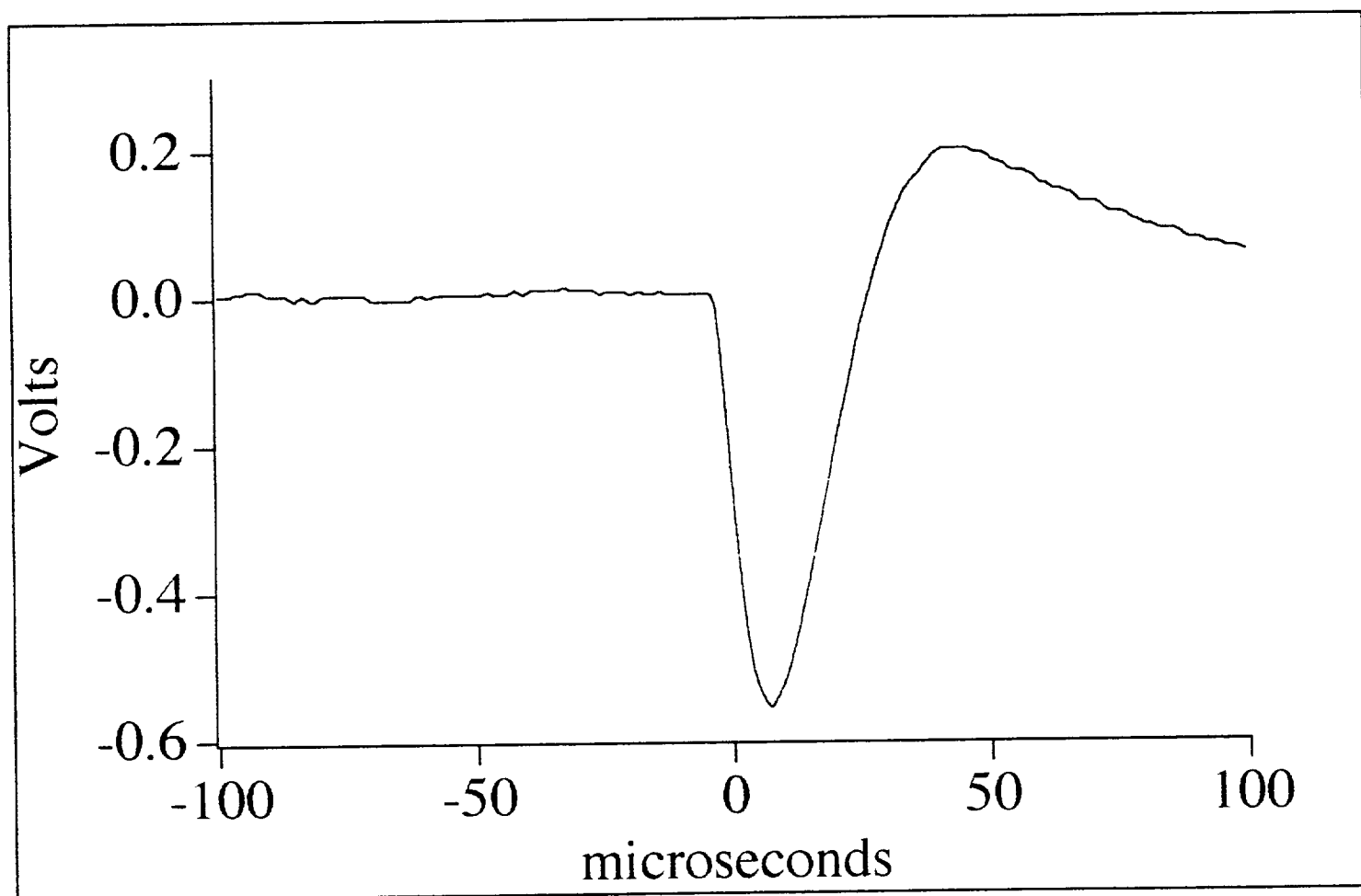Figure 1 : DC Current – Voltage Trace at T=0.3 K

Figure 2 : Typical Pulse Shape of
Integrated Charge

* from a *single* 6 keV x-ray

Figure 3: Energy Spectrum from 6 keV x-rays
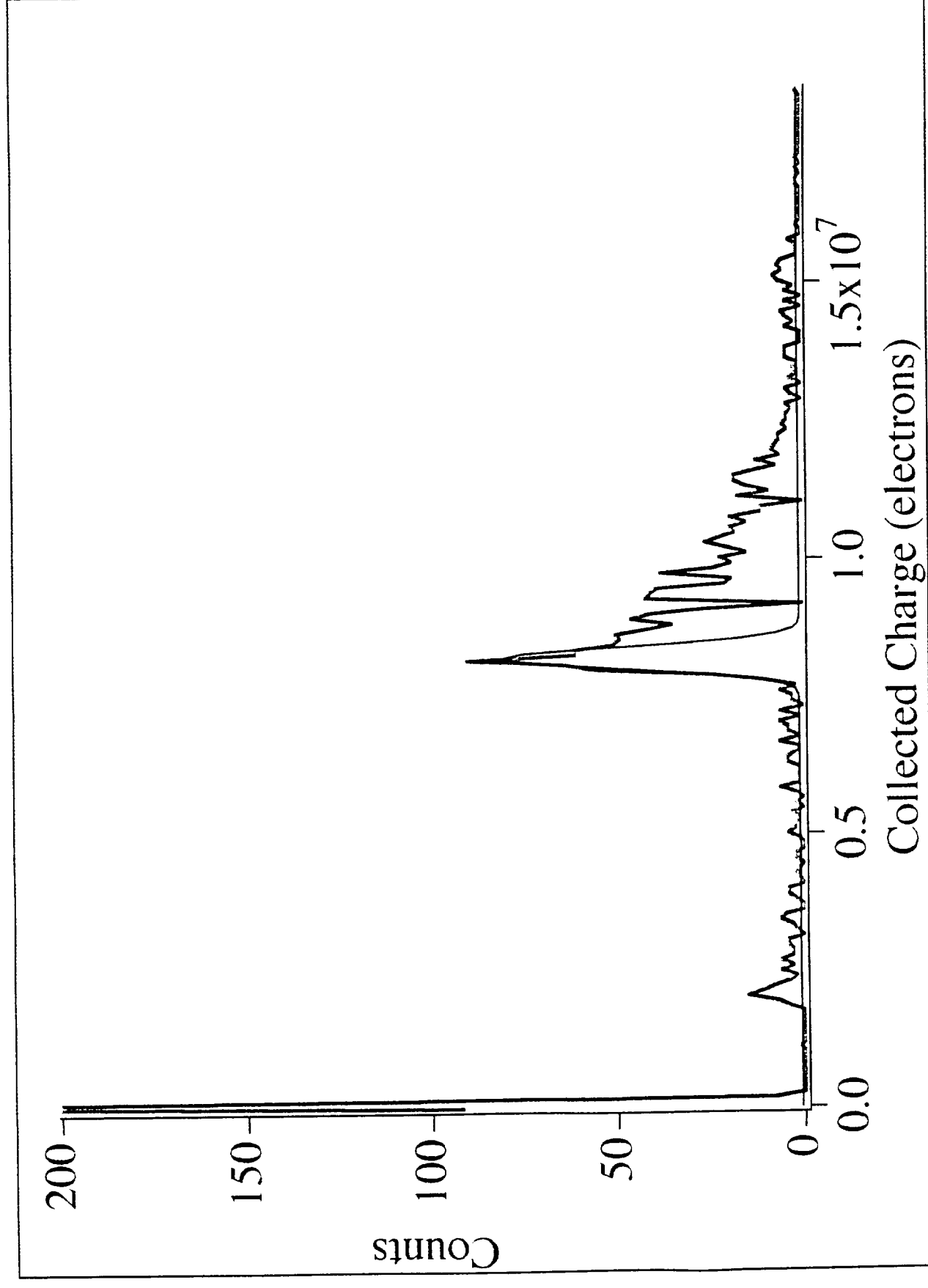
Gaussian fit: FWHM = 350 eV

Figure 4: Integrated Pulse Risetime Histogram
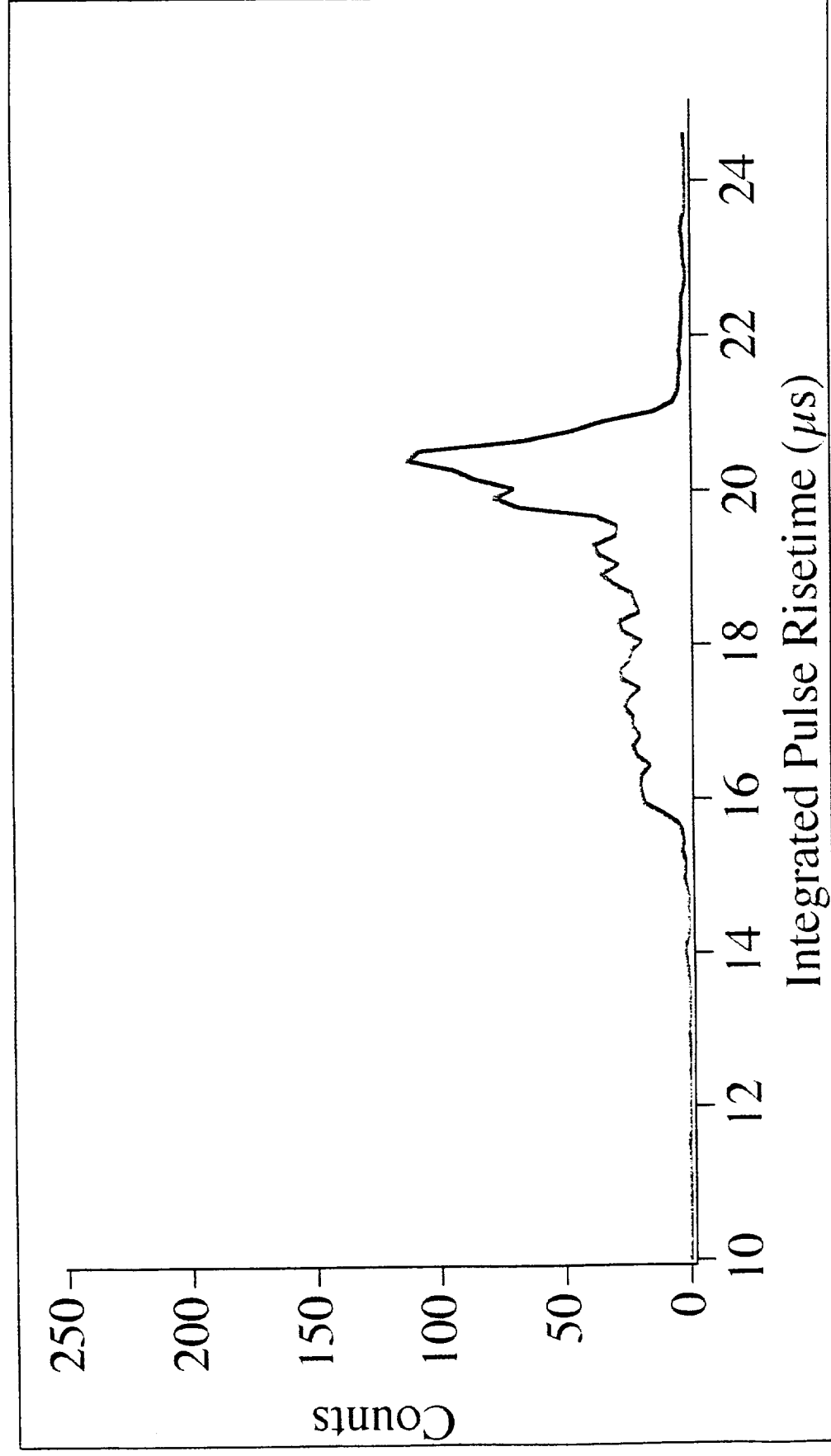
Figure 5: Energy Spectrum (no fast pulses)
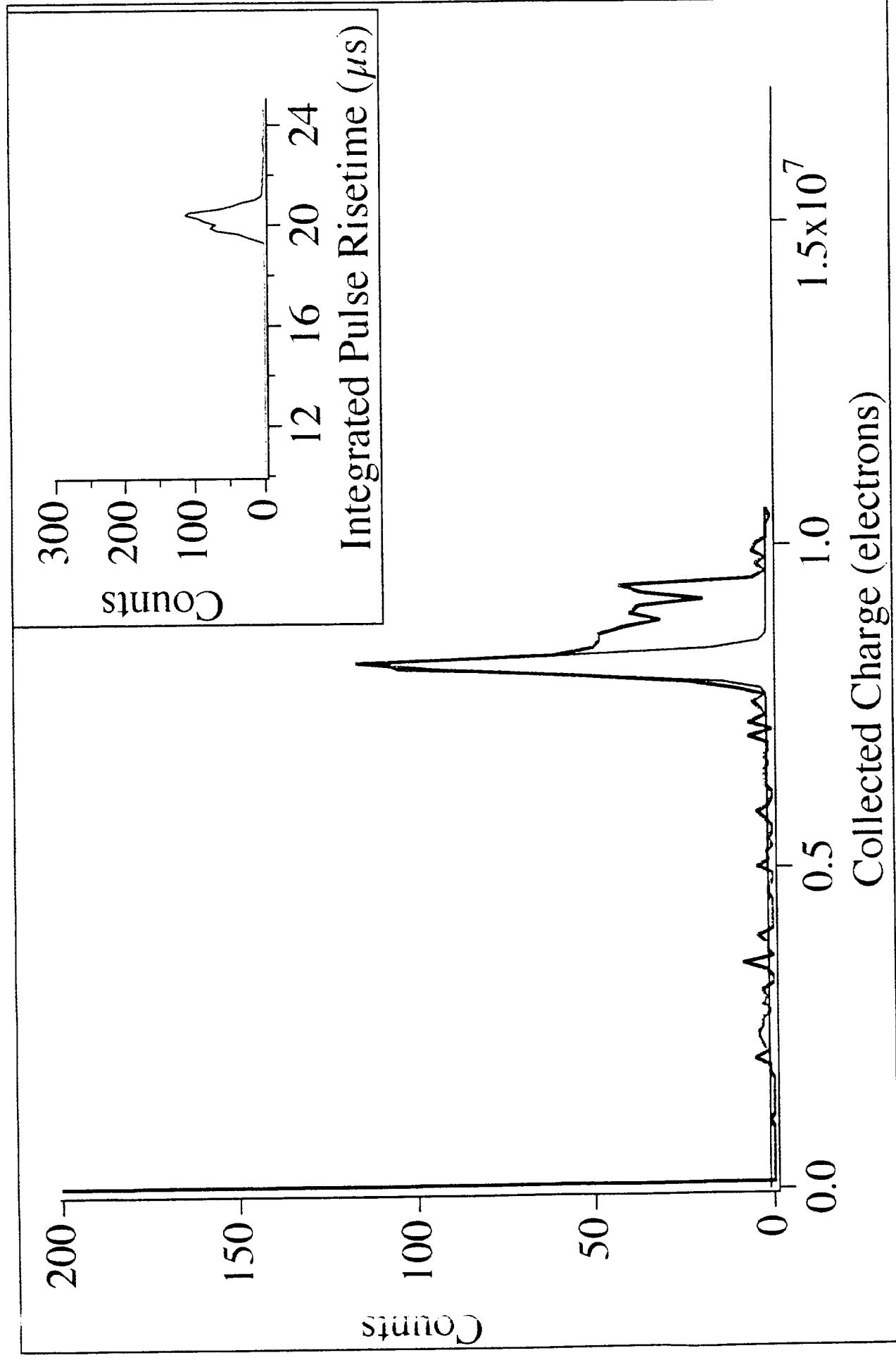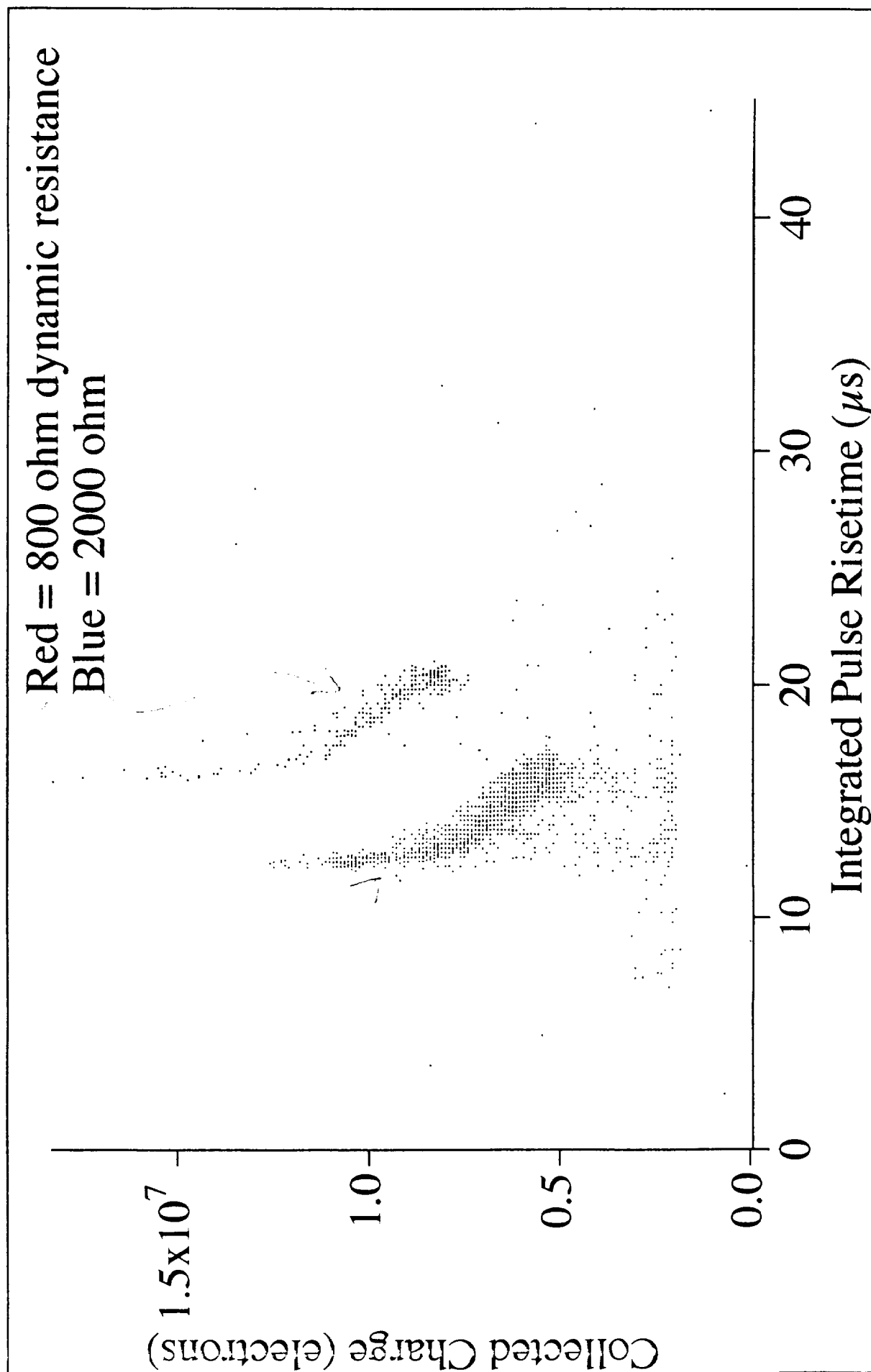
Gaussian Fit: FWHM ≈ 230 eV, for 6 keV x-rays

Figure 7: Junction Dynamic Resistance
Effects on Charge Collection

Red = 800 ohm dynamic resistance
Blue = 2000 ohm